Numerical relativity and binary black holes

Eric Gourgoulhon
Département d'Astrophysique Relativiste et de Cosmologie
CNRS / Observatoire de Paris
Meudon, France

Based on a collaboration with
Silvano Bonazzola, Philippe Grandclément, Jérôme Novak

Jean-Alain Marck

1955 - 2000

1. Einstein equations in 3+1 form *(the equations to be solved)*
2. Numerical methods *(multi-domain spectral methods)*
3. Binary black holes on circular orbits *(a new formulation)*
4. Numerical results *(and comparison with 3-PN)*

Einstein equations in 3+1 form

(the equations to be solved)

3+1 formalism of general relativity

Slicing of spacetime by a family of spacelike hypersurfaces Σ_t.

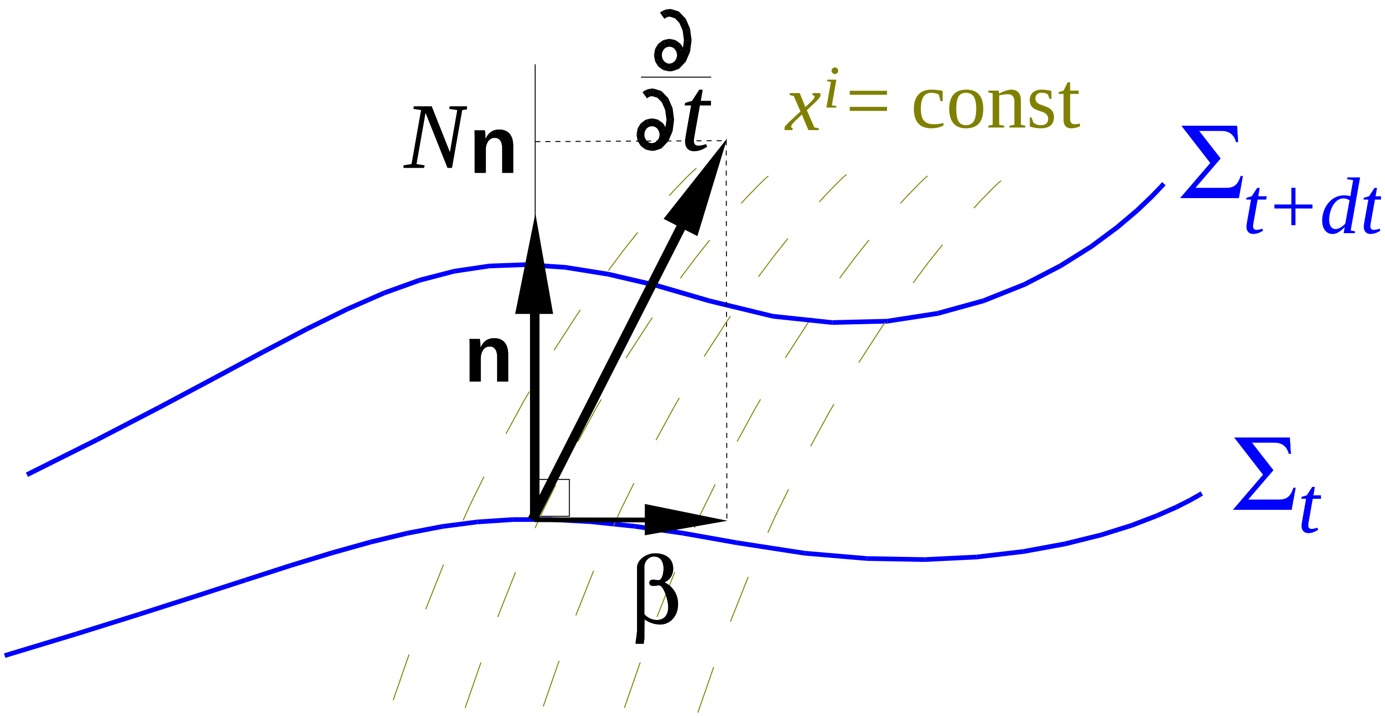

$\mathbf{n}$: unit normal to Σ_t ($\mathbf{n} = -N\nabla t$)

N : lapse function, $\boldsymbol{\beta}$: shift vector

$\frac{\partial}{\partial t} = N\mathbf{n} + \boldsymbol{\beta}$ with $\mathbf{n} \cdot \boldsymbol{\beta} = 0$

3-metric $\boldsymbol{\gamma}$ induced by the spacetime metric $\mathbf{g}$ onto the hypersurfaces Σ_t:

$$\boldsymbol{\gamma} = \mathbf{g} + \mathbf{n} \otimes \mathbf{n}$$

Components of the metric tensor expressed in terms of the lapse function and the components of the shift vector and the 3-metric:

$$g_{\mu\nu} dx^\mu dx^\nu = -(N^2 - \beta_i \beta^i)\, dt^2 + 2\beta_i \, dt \, dx^i + \gamma_{ij} \, dx^i \, dx^j$$

Extrinsic curvature tensor $\mathbf{K}$ of the hypersurface Σ_t

$$\mathbf{K} = -\frac{1}{2} \pounds_{\mathbf{n}} \boldsymbol{\gamma}$$

(Lie derivative of the 3-metric along the flow normal to Σ_t)

Vacuum Einstein equations within the 3+1 formalism

- Hamiltonian constraint: $R + K^2 - K_{ij}K^{ij} = 0$
- Momentum constraint: $D_j K^{ij} - D^i K = 0$
- "Dynamical" equations:

$$\frac{\partial K_{ij}}{\partial t} - \pounds_{\boldsymbol{\beta}} K_{ij} = -D_i D_j N + N \left(R_{ij} - 2K_{ik}K^k_{\ j} + K K_{ij} \right) \ ,$$

$$\frac{\partial \gamma_{ij}}{\partial t} - \pounds_{\boldsymbol{\beta}} \gamma_{ij} = -2N K_{ij}$$

(R_{ij} : Ricci tensor of the 3-metric $\boldsymbol{\gamma}$, D_i : covariant derivative associated with $\boldsymbol{\gamma}$)

Numerical methods

Multi-domain spectral methods

Spectral methods versus finite differences

Spectral method: represent a given function (physical scalar or tensorial field) u by another *function* $I\,u$ belonging to a certain vectorial space of finite dimension $\mathcal{H}$.

Finite differences: represent a physical function u by a finite set of *numbers*: the values $(u_1, \ldots, u_n)$ taken by u at some grid points $(x_1, \ldots, x_n)$.

This fundamental difference — function vs. numbers — is the reason why spectral methods are usually much more precise than finite difference methods.

Spectral expansions

Physical fields : Hilbert space $\mathcal{W}$ (typically a L^2 space)

Vectorial space $\mathcal{H}$ of the spectral method : chosen to be a finite dimensional sub-space of the Hilbert space $\mathcal{W}$

$(\varphi_0, \ldots, \varphi_N)$: orthonormal basis of $\mathcal{H}$

Orthogonal projection of u onto $\mathcal{H}$:

$$P\,u = \sum_{n=0}^{N} \tilde{u}_n \varphi_n$$

Coefficients $(\tilde{u}_0, \ldots, \tilde{u}_N)$ given by the scalar product within $\mathcal{W}$ of u with the basis functions:

$$\tilde{u}_n = \langle u, \varphi_n \rangle$$

Aliasing error

Usually the scalar product $\langle u, \varphi_n \rangle$ involves an integral which cannot be computed exactly. For this reason, the representation of u within the spectral method is not $P\,u$ but a function

$$I\,u = \sum_{n=0}^{N} \hat{u}_n \varphi_n \ ,$$

where the coefficients $\hat{u}_n$ are some approximations of the coefficients $\tilde{u}_n$. The difference between $\tilde{u}_n$ and $\hat{u}_n$ is called the *aliasing error* (contamination of $\hat{u}_n$ by the high frequencies $\tilde{u}_k$ with $k > N$).

For the spectral method, the function u is entirely described by the set of its coefficients $(\hat{u}_0, \ldots, \hat{u}_N)$.

Evaluation of linear operators

Any linear operation on u, such as a partial derivative, amounts to a *matrix multiplication* in the coefficient space. Indeed, if L is a linear operator

$$L \cdot I\, u = \sum_{n=0}^{N} \hat{u}_n \; L \cdot \varphi_n = \sum_{k=0}^{N} \left(\sum_{n=0}^{N} a_{kn} \hat{u}_n \right) \varphi_k \ ,$$

where the coefficients a_{kn} are defined by

$$L \cdot \varphi_n = \sum_{k=0}^{N} a_{kn} \varphi_k \ .$$

Multi-domain spectral methods

Multi-domain spectral methods for 3-D numerical relativity have been introduced in *Bonazzola, Gourgoulhon & Marck, Phys. Rev. D* **58***, 104020 (1998)*.

The computational domain is covered by a *set of domains*; in each domain, basis functions are chosen and spectral expansions are performed.

Example: set of spherical domains covering the entire space

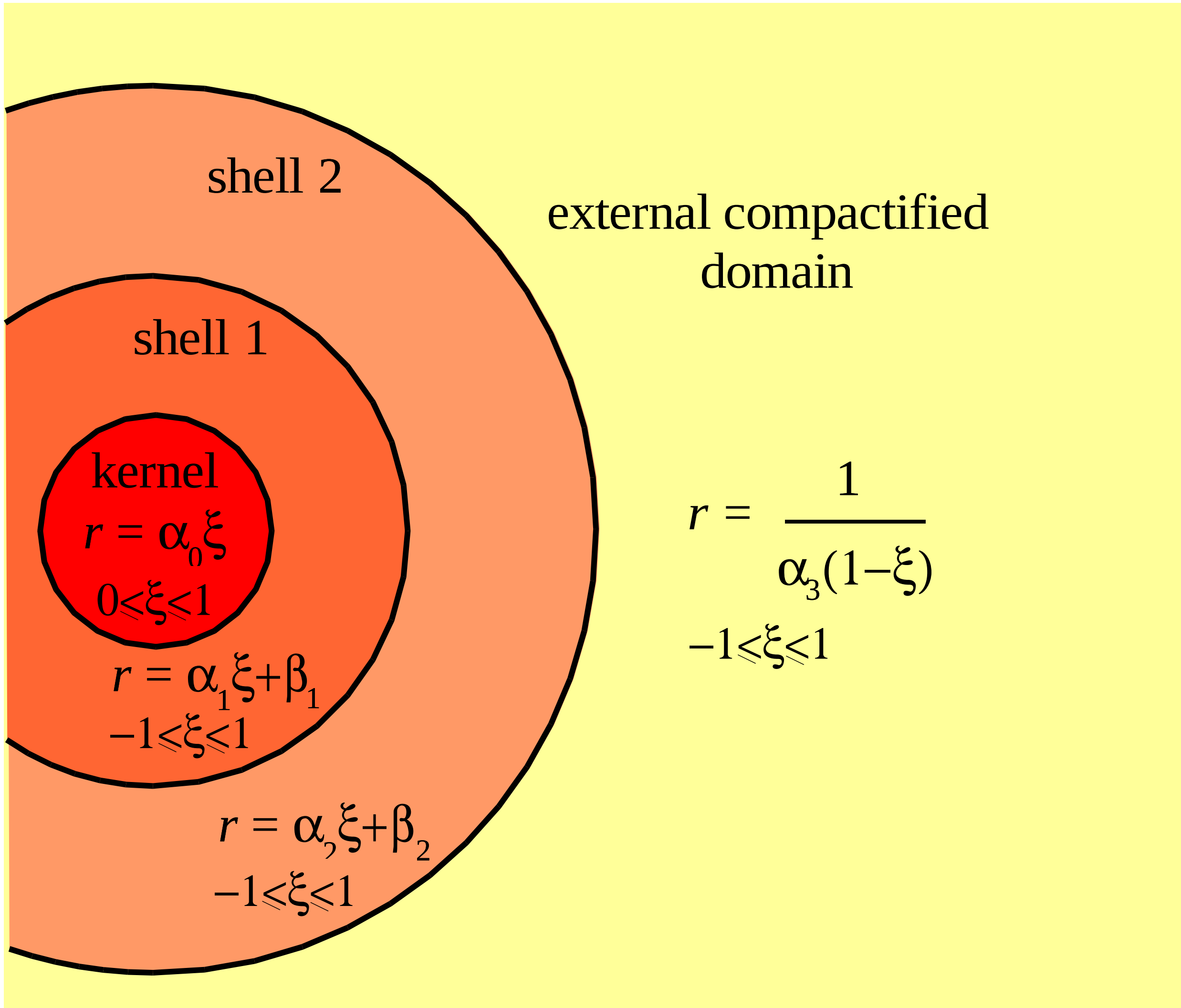

physical coordinates

(r, θ, φ)

comput. coordinates

(ξ, θ, φ)

Sets of domains for a binary system

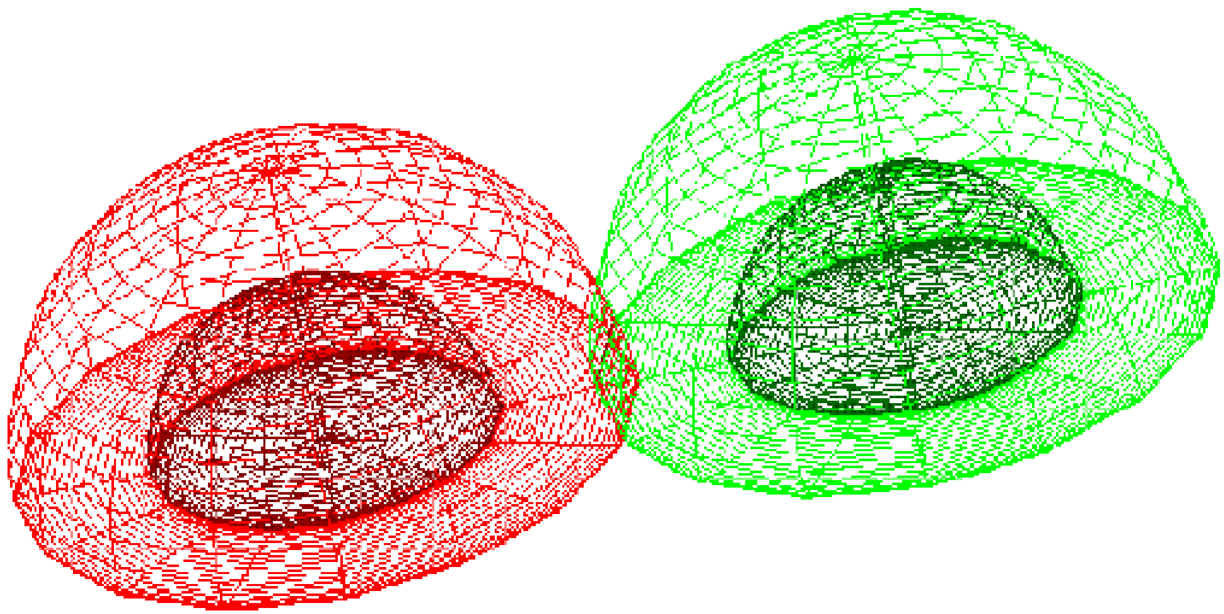

Basis functions for the spectral expansions

$$u(\xi,\theta,\varphi) = \sum_{m=0}^{N_\varphi/2} \sum_{j=0}^{N_\theta-1} \sum_{i=0}^{N_r-1} \hat{u}_{mji}\ X_i(\xi)\ \Theta_j(\theta)\ e^{im\varphi}$$

Regularity at the origin and on the axis $\theta = 0$ + equatorial symmetry:

- φ expansion: *Fourier series*
- θ expansion: *Trigonometric polynomials* or *associated Legendre functions*
  - for m even: $\Theta_j(\theta) = \cos(2j\theta)$ or $\Theta_j(\theta) = P_{2j}^m(\cos\theta)$
  - for m odd: $\Theta_j(\theta) = \sin((2j+1)\theta)$ or $\Theta_j(\theta) = P_{2j+1}^m(\cos\theta)$
- ξ expansion: *Chebyshev polynomials*
  - in the kernel: $X_i(\xi) = T_{2i}(\xi)$ for m even, $X_i(\xi) = T_{2i+1}(\xi)$ for m odd
  - in the shells and the external compactified domain: $X_i(\xi) = T_i(\xi)$

Resolution of elliptic equations with non-compact sources

Maximal slicing: $\Delta N = S$

Minimal distortion equation for the shift vector: $\Delta\boldsymbol{\beta} + \frac{1}{3}\nabla(\nabla\cdot\boldsymbol{\beta}) = \mathbf{S}$

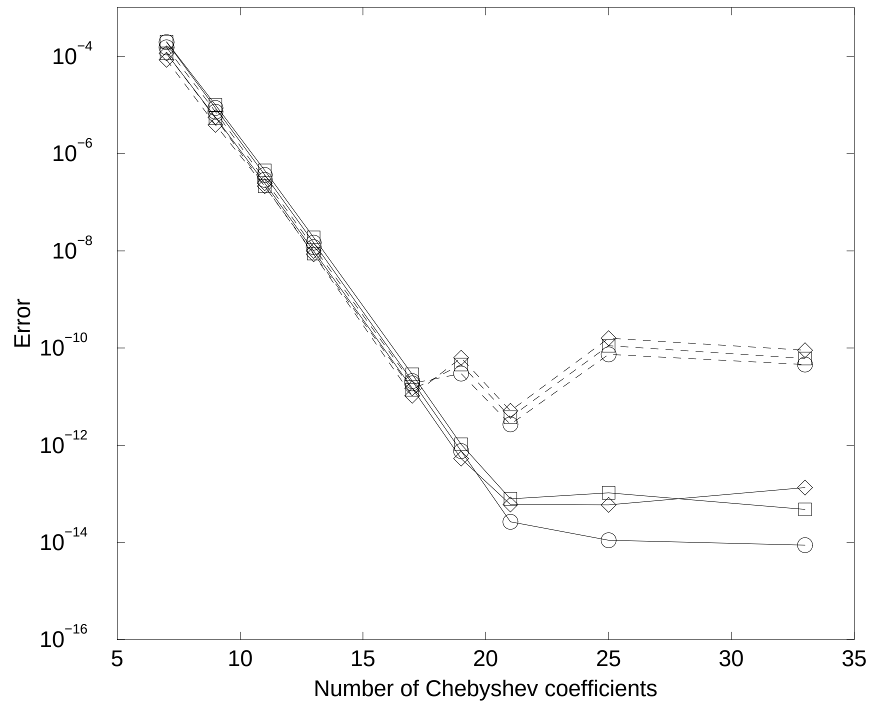

Error on the z component of the solution of the minimal distortion equation with a non-compact source

Grandclément, Bonazzola, Gourgoulhon & Marck, J. Comp. Phys. **170**, *231 (2001)*.

Behavior of the numerical error in solving Poisson-type equations

- Source with a *compact support*: evanescent error, i.e. error $\propto \exp(-N_r)$
- Source with a *non-compact support*, decaying as r^{-k}:
  - evanescent error if the source does not contain any spherical harmonics of index $\ell \geq k-3$ (scalar case) or $\ell \geq k-5$ (vectorial case)
  - error decreasing as $N^{-2(k-2)}$ otherwise

Adaptive domains

General mapping for starlike domains:

$$r = \alpha[\xi + A(\xi)F(\theta', \varphi') + B(\xi)G(\theta', \varphi')] + \beta, \quad \theta = \theta', \quad \varphi = \varphi'$$

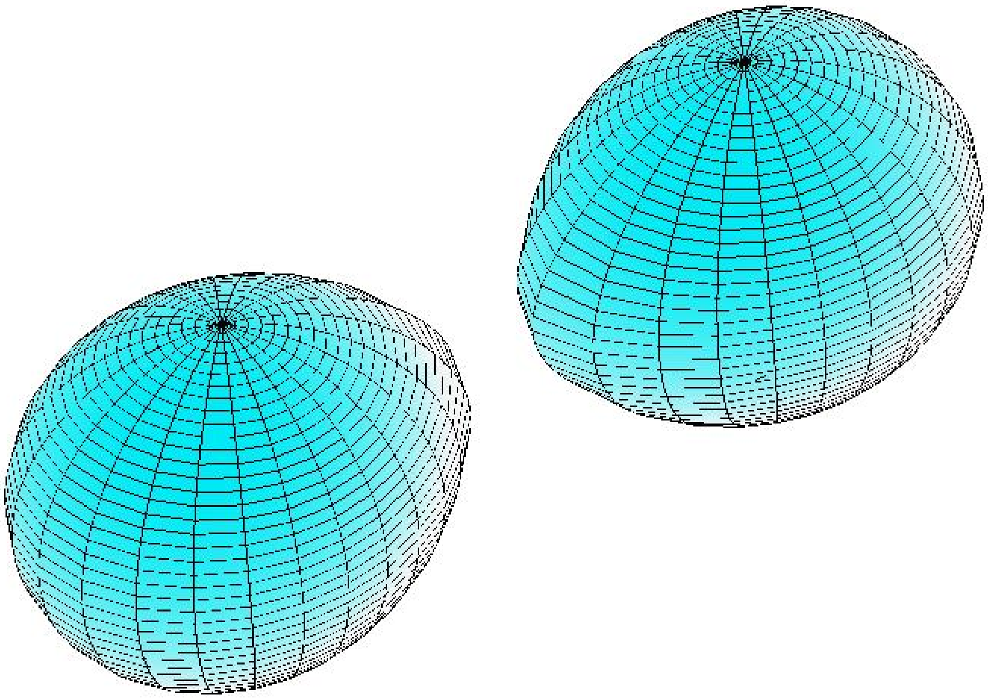

Application to binary neutron stars (surface-fitted coordinates)

Gourgoulhon, Grandclément, Taniguchi, Bonazzola & Marck, Phys. Rev. D **63**, *064029 (2001)*
Taniguchi, Gourgoulhon & Bonazzola, Phys. Rev. D **64**, *064012 (2001)*
Taniguchi & Gourgoulhon, astro-ph/0108086

Numerical implementation

Object-oriented languages (C++, Ada, Java, ...) are much more efficient than procedural languages (Fortran, C, ...) when treating complex problems.

Our choice (Jean-Alain Marck 1997): C++

C++ based language developed in Meudon:

LORENE (*L*angage *O*bjet pour la *RE*lativité *N*umériqu*E*)

Binary black holes

on circular orbits

Problem treated:

Binary black holes in the pre-coalescenge stage

$\Rightarrow$ the notion of *orbit* has still some meaning

Basic idea:

Construct an approximate, but full spacetime (i.e. *4-dimensional*) representing 2 orbiting black holes

Previous numerical treatments: 3-dimensional (initial value problem on a spacelike 3-surface)

4-dimensional approach $\Rightarrow$ rigorous definition of orbital angular velocity

First results:

Gourgoulhon, Grandclément & Bonazzola, gr-qc/0106015.

Grandclément, Gourgoulhon & Bonazzola, gr-qc/0106016.

Spacetime manifold

Topology : $\mathbf{R} \times$ Misner-Lindquist

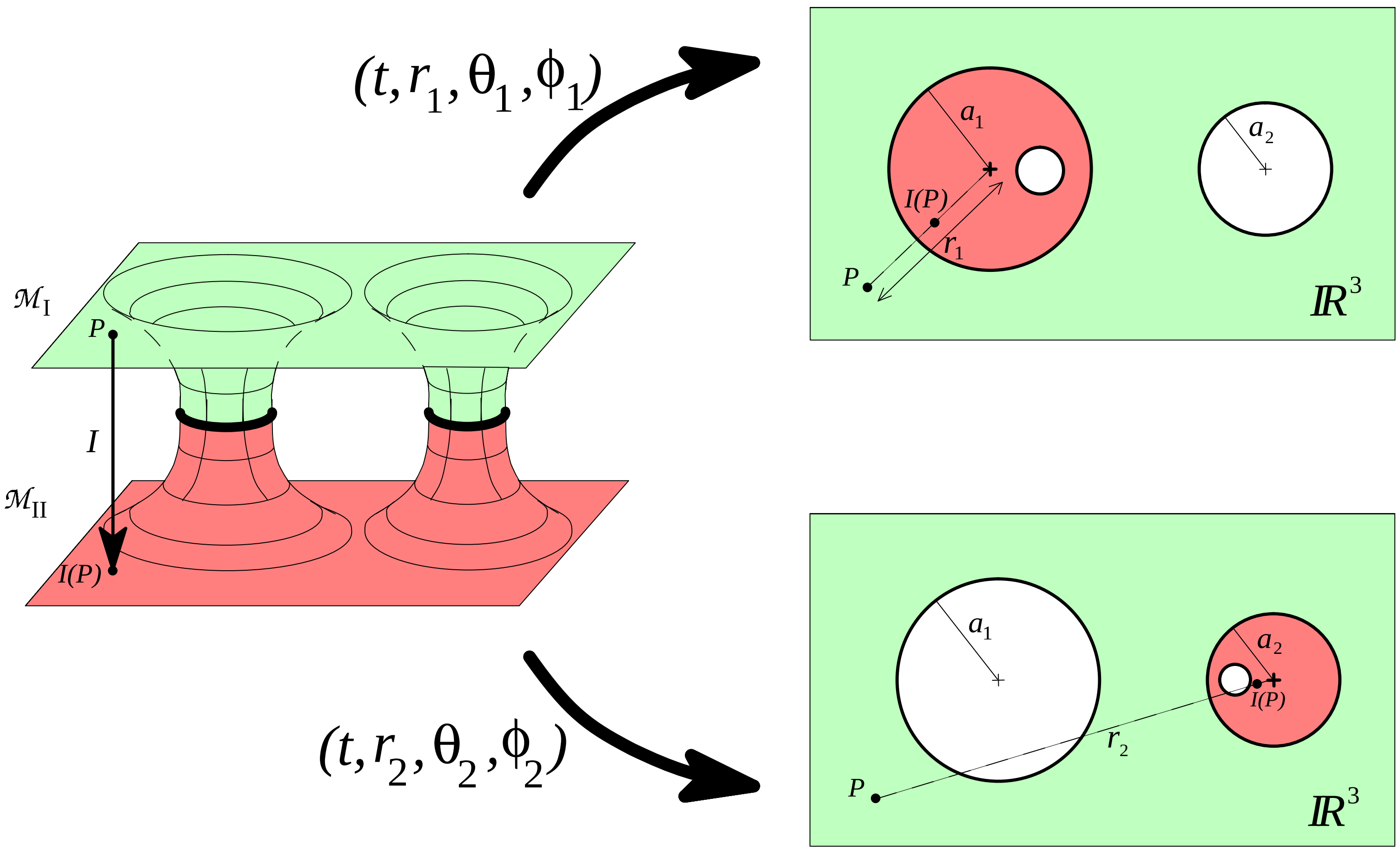

Canonical mapping: $I: \quad (t, r_1, \theta_1, \varphi_1) \mapsto \left(t, \frac{a_1^2}{r_1}, \theta_1, \varphi_1\right)$

Isometry between the two sheets

Assumption: the canonical mapping I is an isometry: $I_*\mathbf{g} = \mathbf{g}$

Consequences:

- $I_* t = t$ and $I_* \nabla t = \nabla t$
- $I_* \mathbf{n} = \pm\mathbf{n}$
- $I_* N = \pm N$ (same sign as **n**)
- $I_* \boldsymbol{\beta} = \boldsymbol{\beta}$
- $I_* \boldsymbol{\gamma} = \boldsymbol{\gamma}$
- $I_* \mathbf{K} = \pm\mathbf{K}$ (same sign as **n**)

Choice of the minus sign

Two families of maximal slicing of the Schwarzschild spacetime:

$+$ sign (symmetric lapse)

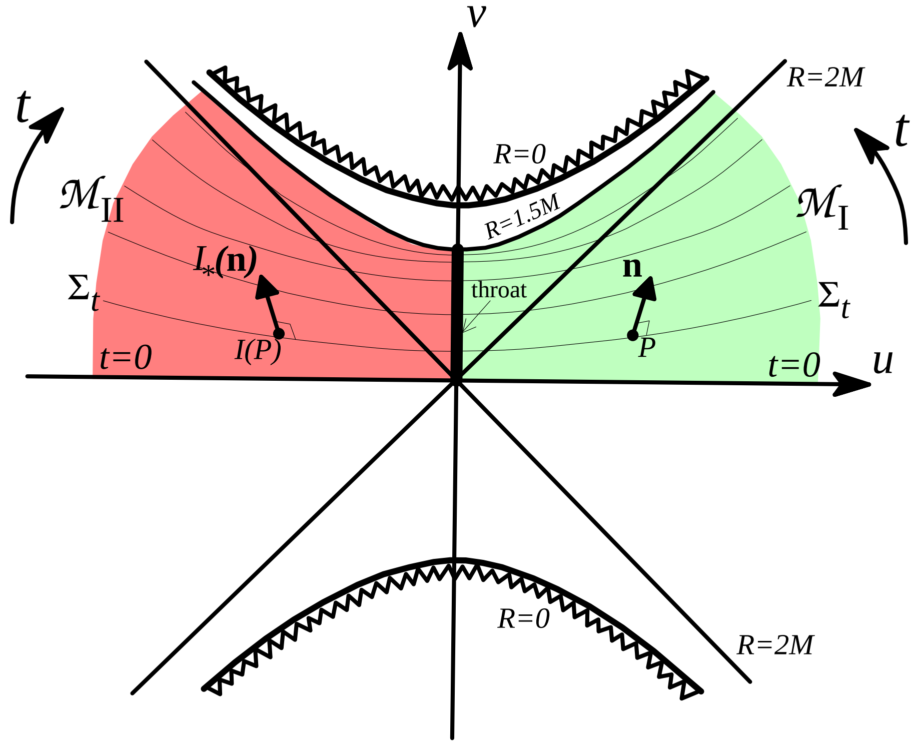

time evolving

$-$ sign (antisymmetric lapse)

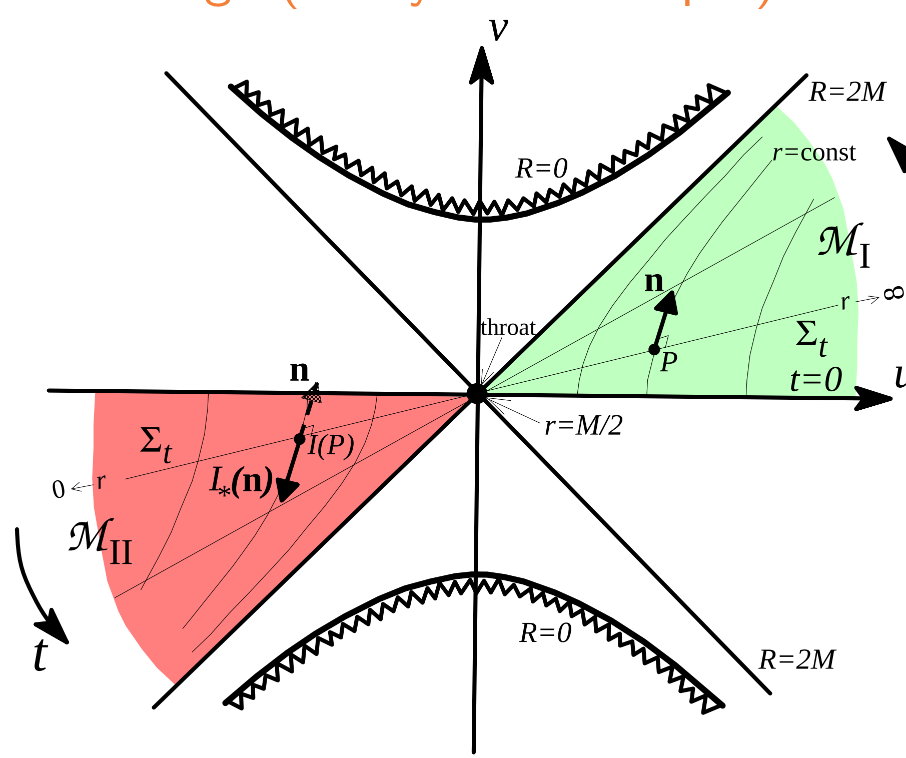

preserves the stationarity

Helical symmetry

Physical assumption: when the two holes are sufficiently far apart, the radiation reaction can be neglected $\Rightarrow$ closed orbits
Gravitational radiation reaction circularizes the orbits $\Rightarrow$ circular orbits

Geometrical translation: there exists a Killing vector field $\boldsymbol{\ell}$ such that:

(i) far from the system (asymptotically inertial coordinates $(t_0, r_0, \theta_0, \varphi_0)$),

$$\boldsymbol{\ell} \rightarrow \frac{\partial}{\partial t_0} + \Omega \frac{\partial}{\partial \varphi_0}$$

(ii) $\boldsymbol{\ell} = \dfrac{\partial}{\partial t}$ ($\Rightarrow \boldsymbol{\ell}$ preserves the throats)

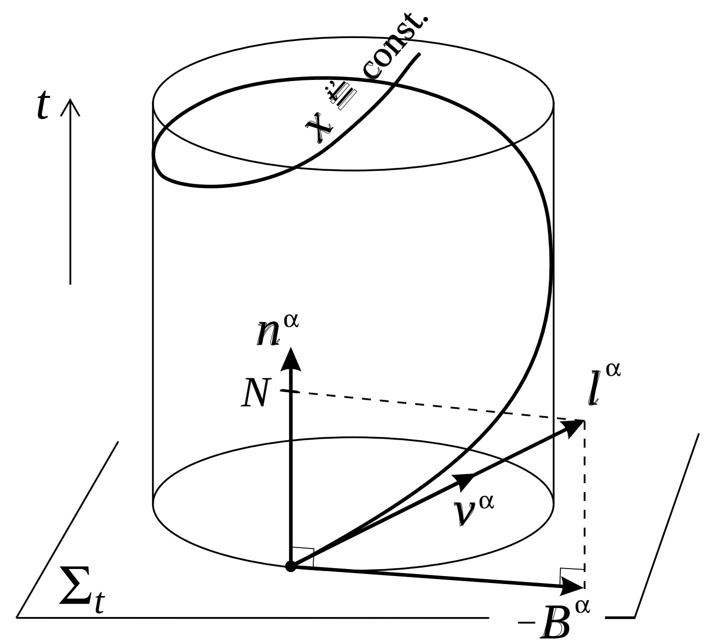

Discussion

Helical symmetry is exact

- in *Newtonian gravity* and in *2nd order Post-Newtonian gravity*
- in general relativity for a non-axisymmetric system (binary) only with *standing gravitational waves*

But a spacetime with a helical Killing vector and standing gravitational waves cannot be asymptotically flat (*Gibbons & Stewart 1983*).

Rotation state of each black hole

Choice: rotation synchronized with the orbital motion (corotating system)

Geometrical translation: the two throats are Killing horizons associated with $\boldsymbol{\ell}$:

$$\boldsymbol{\ell} \cdot \boldsymbol{\ell}|_{\mathcal{S}_1} = 0 \qquad \text{and} \qquad \boldsymbol{\ell} \cdot \boldsymbol{\ell}|_{\mathcal{S}_2} = 0 \; .$$

[cf. the rigidity theorem for a Kerr black hole]

Consequence on the shift vector:

$$\boldsymbol{\ell} \cdot \boldsymbol{\ell} = -N^2 + \boldsymbol{\beta} \cdot \boldsymbol{\beta}$$

Since (choice of the minus sign in the isometry condition for the lapse) $N|_{\mathcal{S}_i} = 0$, the shift vector must vanish on the throats:

$$\boldsymbol{\beta}|_{\mathcal{S}_1} = 0 \qquad \text{and} \qquad \boldsymbol{\beta}|_{\mathcal{S}_2} = 0 \; .$$

Einstein equations

Assumption: Maximal slicing: $K = 0$

Approximation: conformally flat spatial metric: $\boldsymbol{\gamma} = \Psi^4 \mathbf{f}$

Amounts to solve 5 of the 10 Einstein equations:

$$\Delta\Psi = -\frac{\Psi^5}{8}\hat{A}_{ij}\hat{A}^{ij} \qquad \textit{(Hamiltonian constraint)}$$

$$\Delta\beta^i + \frac{1}{3}\bar{D}^i\bar{D}_j\beta^j = 2\hat{A}^{ij}\left(\bar{D}_jN - 6N\bar{D}_j\ln\Psi\right) \qquad \textit{(momentum constraint)}$$

$$\Delta N = N\Psi^4\hat{A}_{ij}\hat{A}^{ij} - 2\bar{D}_j\ln\Psi\,\bar{D}^jN \qquad \textit{(trace of } \frac{\partial K_{ij}}{\partial t} = \cdots\textit{)}$$

with $\hat{A}_{ij} := \Psi^{-4}K_{ij}$ and $\hat{A}^{ij} := \Psi^4 K^{ij}$

Kinematical relation between $\boldsymbol{\gamma}$ and $\mathbf{K}$:

$$\hat{A}^{ij} = \frac{1}{2N}(L\beta)^{ij} \qquad \textit{(traceless part)}$$

$$\bar{D}_i\beta^i = -6\beta^i\bar{D}_i\ln\Psi \qquad \textit{(trace part)}$$

with $(L\beta)^{ij} := \bar{D}^i\beta^j + \bar{D}^j\beta^i - \frac{2}{3}\bar{D}_k\beta^k f^{ij}$

Boundary conditions

isometry condition on γ_{rr}:

$$\left.\left(\frac{\partial\Psi}{\partial r_1} + \frac{\Psi}{2r_1}\right)\right|_{\mathcal{S}_1} = 0 \qquad \left.\left(\frac{\partial\Psi}{\partial r_2} + \frac{\Psi}{2r_2}\right)\right|_{\mathcal{S}_2} = 0$$

asymptotic flatness:

$\Psi \to 1$ when $r \to \infty$

corotating black holes:

$$\boldsymbol{\beta}|_{\mathcal{S}_1} = 0 \qquad \boldsymbol{\beta}|_{\mathcal{S}_2} = 0$$

definition of $\boldsymbol{\ell}$:

$\boldsymbol{\beta} \to \Omega \dfrac{\partial}{\partial\varphi_0}$ when $r \to \infty$

isometry condition on N:

$$N|_{\mathcal{S}_1} = 0 \qquad N|_{\mathcal{S}_2} = 0$$

asymptotic flatness:

$N \to 1$ when $r \to \infty$

Regularity on the horizon

Position of the problem:

$$\left.\begin{array}{l} K^{ij} = \dfrac{(L\beta)^{ij}}{2\Psi^4 N} \\ N|_{\mathcal{S}} = 0 \end{array}\right\} \Longrightarrow \text{one must have } L\boldsymbol{\beta}|_{\mathcal{S}} = 0 \text{ for } \mathbf{K} \text{ to be regular}$$

$$\text{One has} \quad \left.\begin{array}{lll} (1) & \boldsymbol{\beta}|_{\mathcal{S}} = 0 & \text{(rigid rotation)} \\ (2) & I_*\boldsymbol{\beta} = \boldsymbol{\beta} & \text{(isometry)} \\ (3) & \bar{D}_i\beta^i = -6\beta^i\bar{D}_i \ln\Psi & (K=0) \end{array}\right\} \Longrightarrow L\boldsymbol{\beta}|_{\mathcal{S}} = 0$$

However, only (1) and the part of (2) implied by (1) are really imposed when solving the vector Poisson equation for $\boldsymbol{\beta}$.

Adopted solution:

Set $\boldsymbol{\beta}_{\rm new} = \boldsymbol{\beta}_{\rm old} + \boldsymbol{\beta}_{\rm cor}$ with $\boldsymbol{\beta}_{\rm cor}$ chosen so that (2) and (3) are fulfilled on the throats.

At the end of the computation, $\boldsymbol{\beta}_{\rm cor}$ must be zero (to get an exact solution) or small (to get an approximate solution).

Determination of Ω

Virial assumption: $O(r^{-1})$ part of the metric ($r \to \infty$) same as Schwarzschild

[The only quantity "felt" at the $O(r^{-1})$ level by a distant observer is the total mass of the system.]

A priori

$$\Psi \sim 1 + \frac{M_{\rm ADM}}{2r} \qquad \text{and} \qquad N \sim 1 - \frac{M_{\rm K}}{r}$$

Hence

$$\text{(virial assumption)} \iff M_{\rm ADM} = M_{\rm K}$$

Note

$$\text{(virial assumption)} \iff \Psi^2 N \sim 1 + \frac{\alpha}{r^2}$$

Link with the classical virial theorem

Einstein equations $\Rightarrow$

$$\Delta \ln(\Psi^2 N) = \Psi^4\left[4\pi S_i^{\ i} + \frac{3}{4}\hat{A}_{ij}\hat{A}^{ij}\right] - \frac{1}{2}\left[\bar{D}_i \ln N \bar{D}^i \ln N + \bar{D}_i \ln(\Psi^2 N)\bar{D}^i \ln(\Psi^2 N)\right]$$

No monopolar $1/r$ term in $\Psi^2 N$ $\iff$

$$\int_{\Sigma_t}\left\{4\pi S_i^{\ i} + \frac{3}{4}\hat{A}_{ij}\hat{A}^{ij} - \frac{1}{2}\Psi^{-4}\left[\bar{D}_i \ln N \bar{D}^i \ln N + \bar{D}_i \ln(\Psi^2 N)\bar{D}^i \ln(\Psi^2 N)\right]\right\}\Psi^4\sqrt{f}\, d^3x = 0$$

Newtonian limit is the classical virial theorem:

$$2E_{\rm kin} + 3P + E_{\rm grav} = 0$$

Defining an evolutionary sequence

An evolutionary sequence is defined by:

$$\left.\frac{dM_{\rm ADM}}{dJ}\right|_{\rm sequence} = \Omega$$

This is equivalent to requiring the constancy of the horizon area of each black hole, by virtue of the First law of thermodynamics for binary black holes :

$$dM_{\rm ADM} = \Omega\, dJ + \frac{1}{8\pi}\left(\kappa_1\, dA_1 + \kappa_2\, dA_2\right)$$

recently established by *Friedman, Uryu & Shibata, gr-qc/0108070*.

Numerical results

Tests passed by the numerical code

Test 1 : obtaining the Schwarzschild solution (single nonrotating black hole)

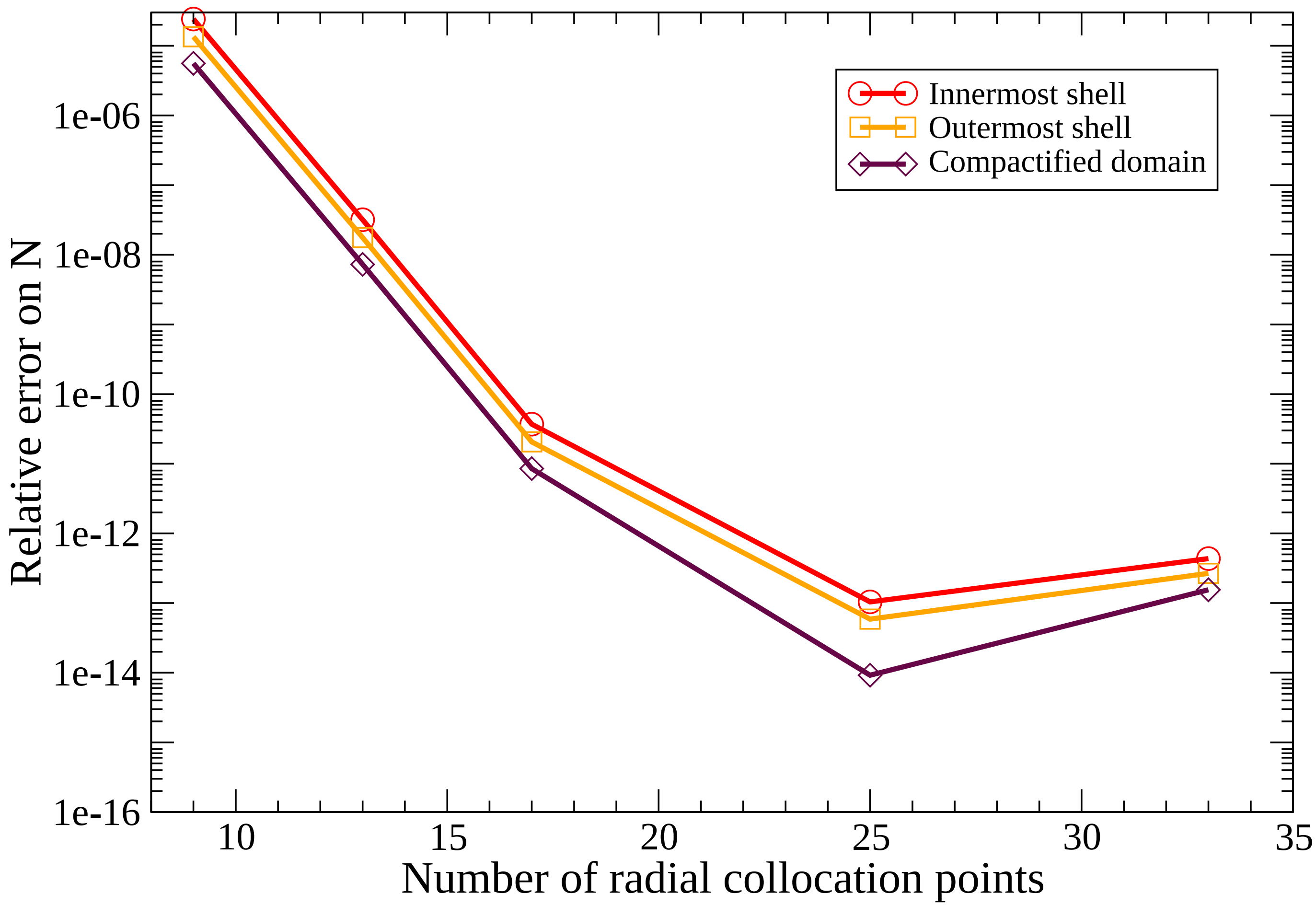

Error on the lapse N as a function of the number of Chebyshev polynomials involved in the radial expansions

Test 2 : obtaining the Kerr solution (single rotating black hole)

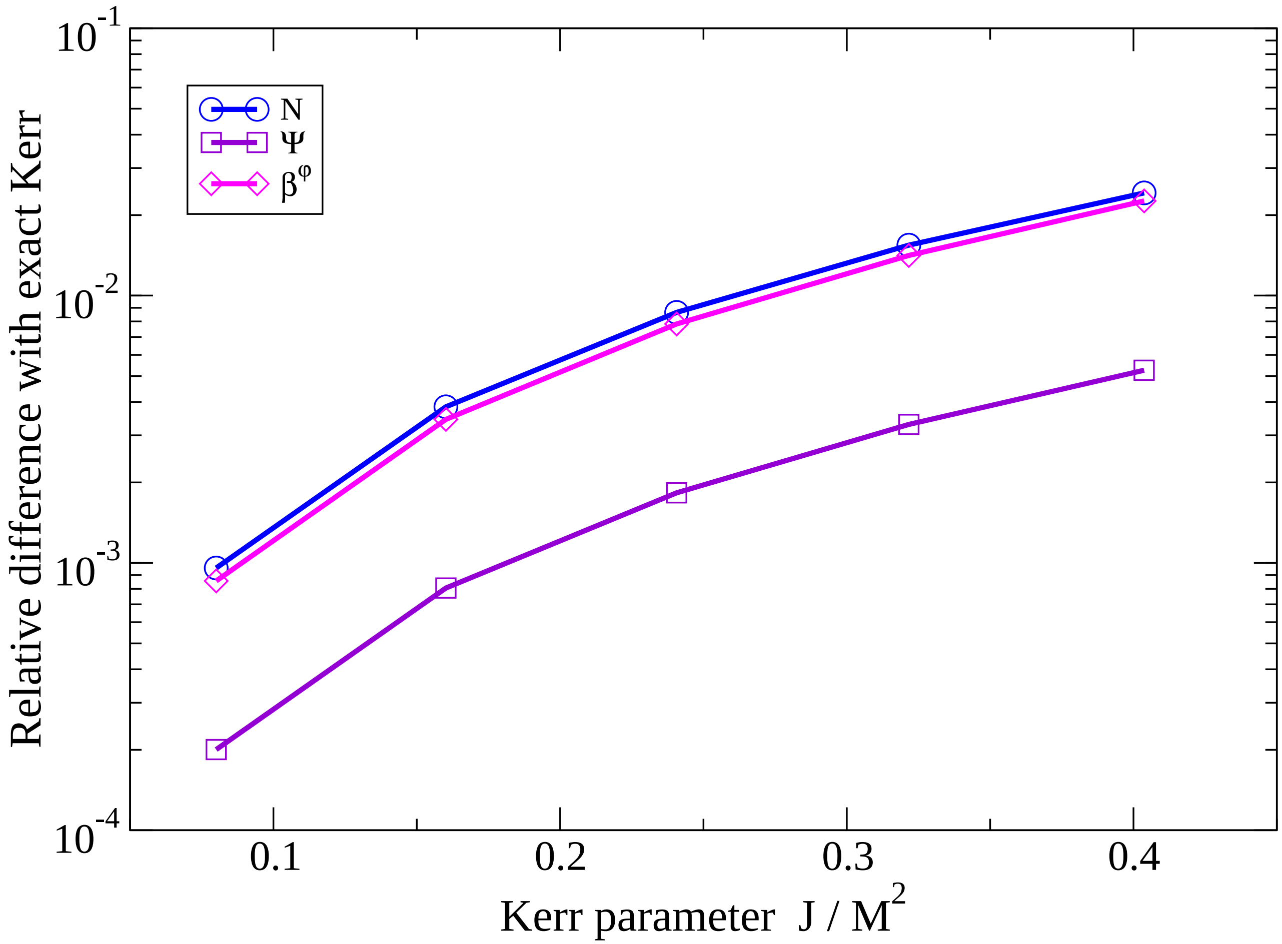

Error on N (circles), Ψ (squares) and β^φ (diamonds) as a function of the Kerr parameter a/M, for $N_r \times N_\theta \times N_\varphi = 25 \times 17 \times 16$ spectral coefficients in each of the 4 domains

Test 3 : obtaining the Misner-Lindquist solution (momentarily static binary black hole)

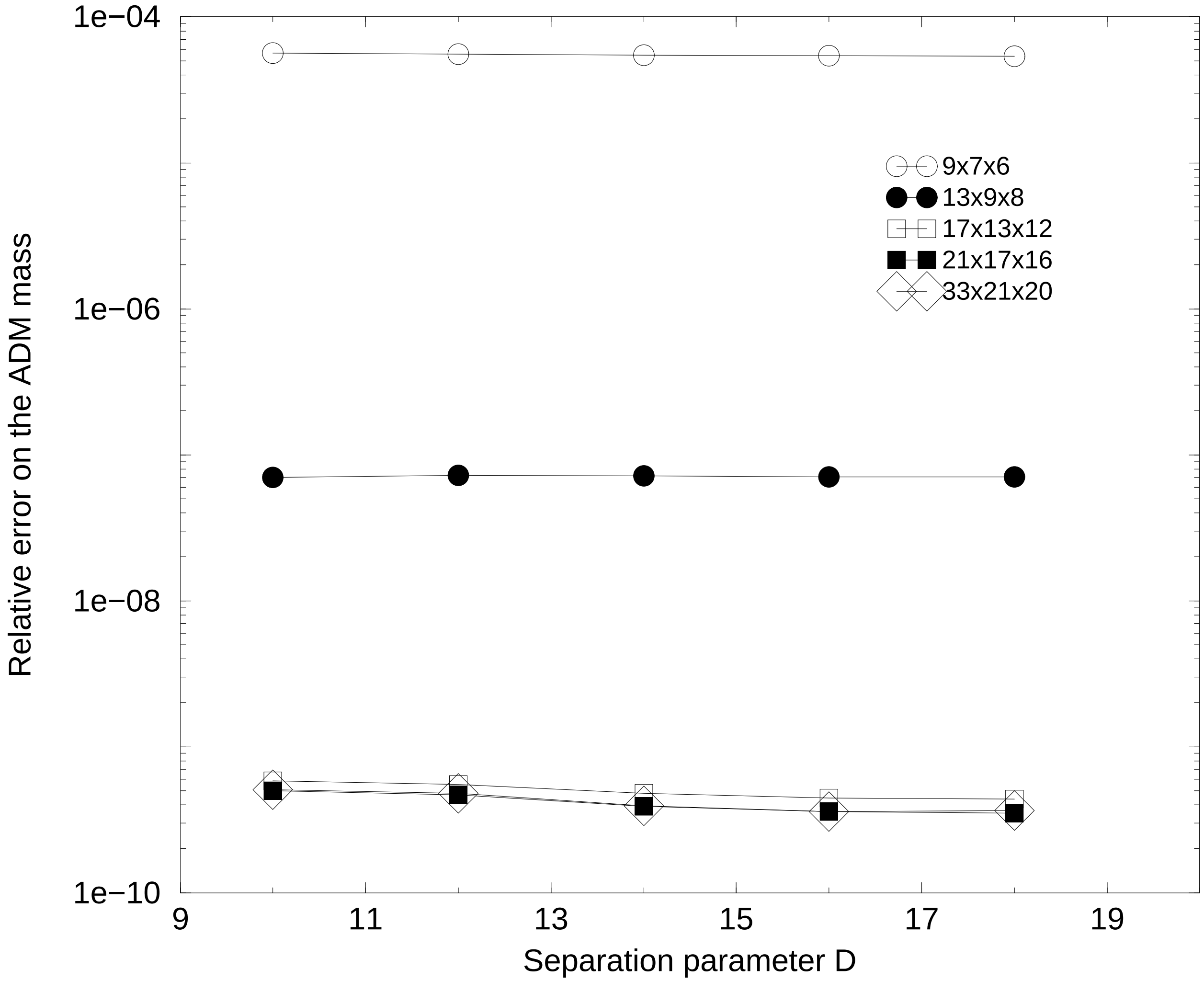

Relative error on the ADM mass

Test 4 : getting Kepler's third law at large separation (binary black hole)

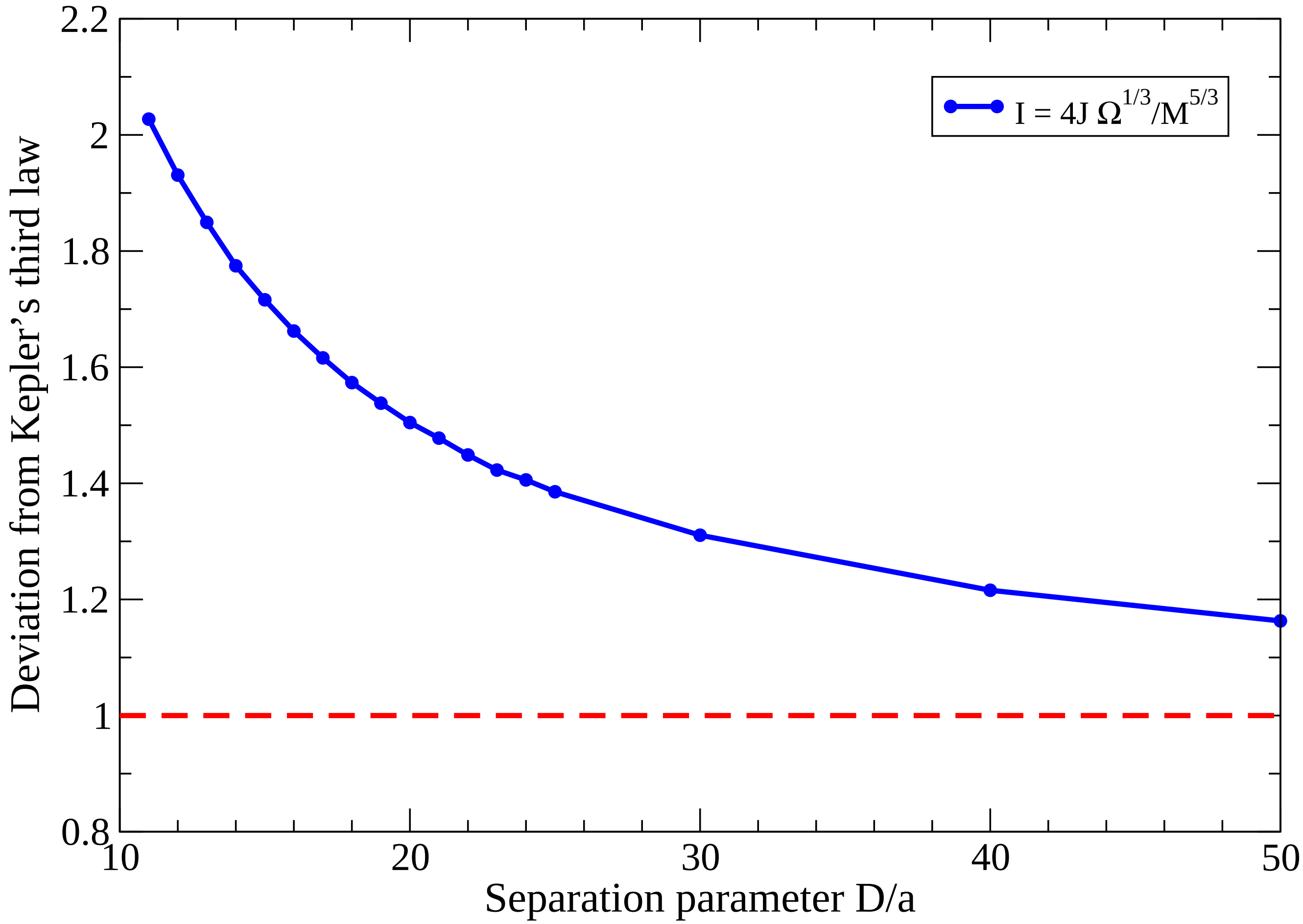

Test 5 : smallness of the correction function on the shift vector

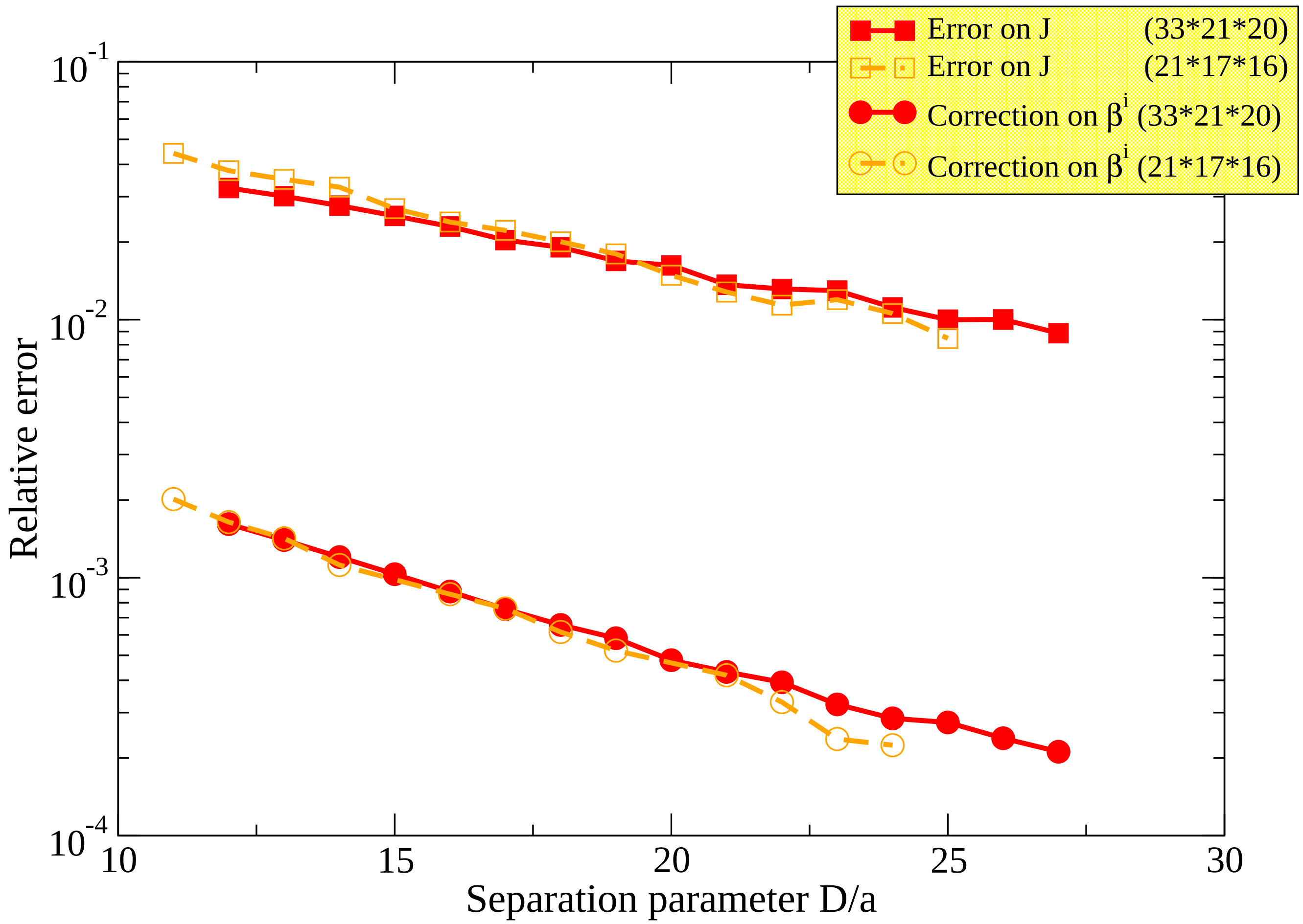

Relative amplitude of the correction function imposed on β and relative difference between the angular momentum J computed at spatial infinity and at the throats

Test 6 : error on Smarr formula

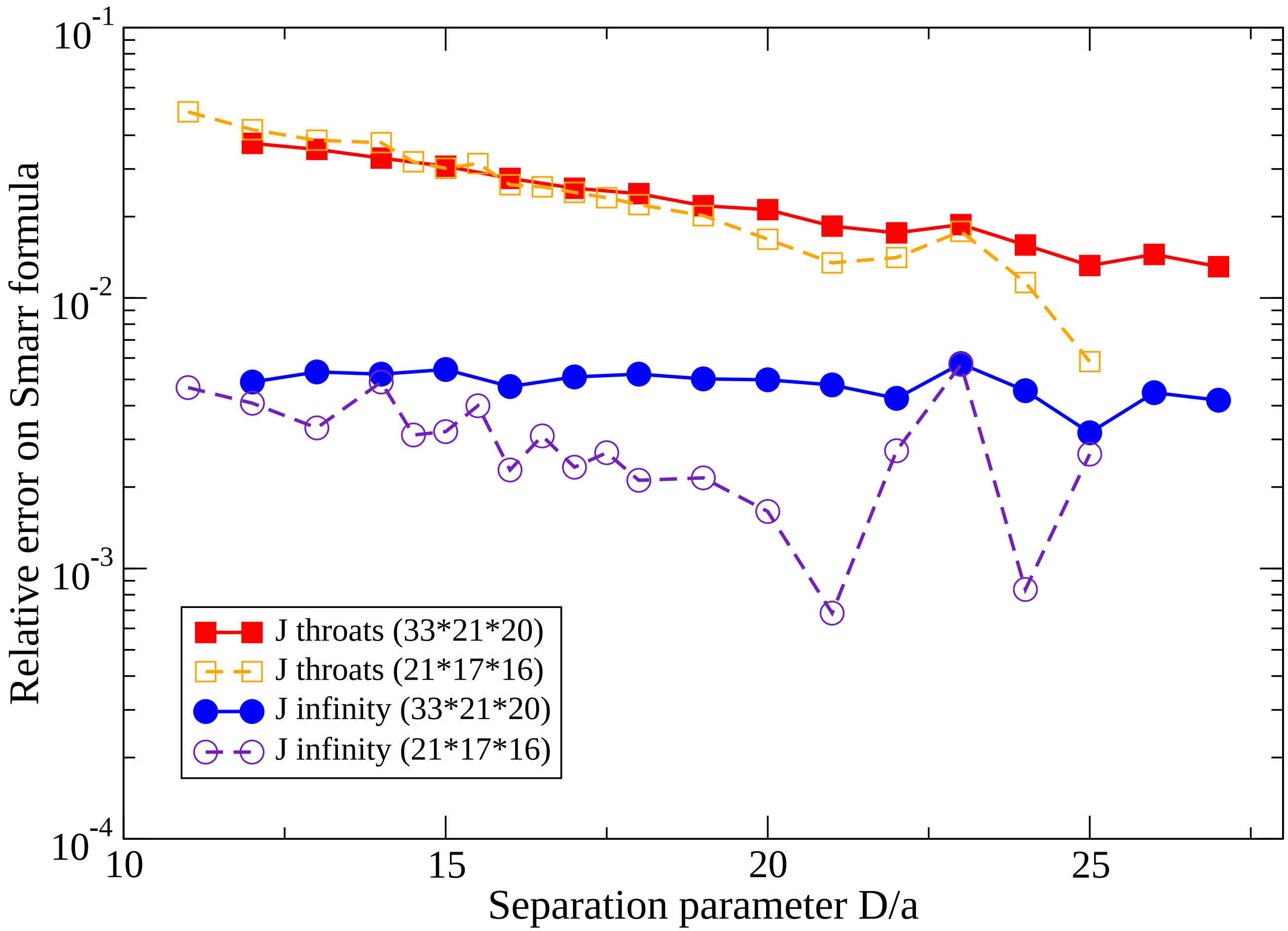

Relative error on Smarr formula $M - 2\Omega J = -1/4\pi \sum_i \oint_{S_i} \Psi^2 \bar{D}_i N \, dS^i$

Test 7 : conservation of the horizon area along a sequence

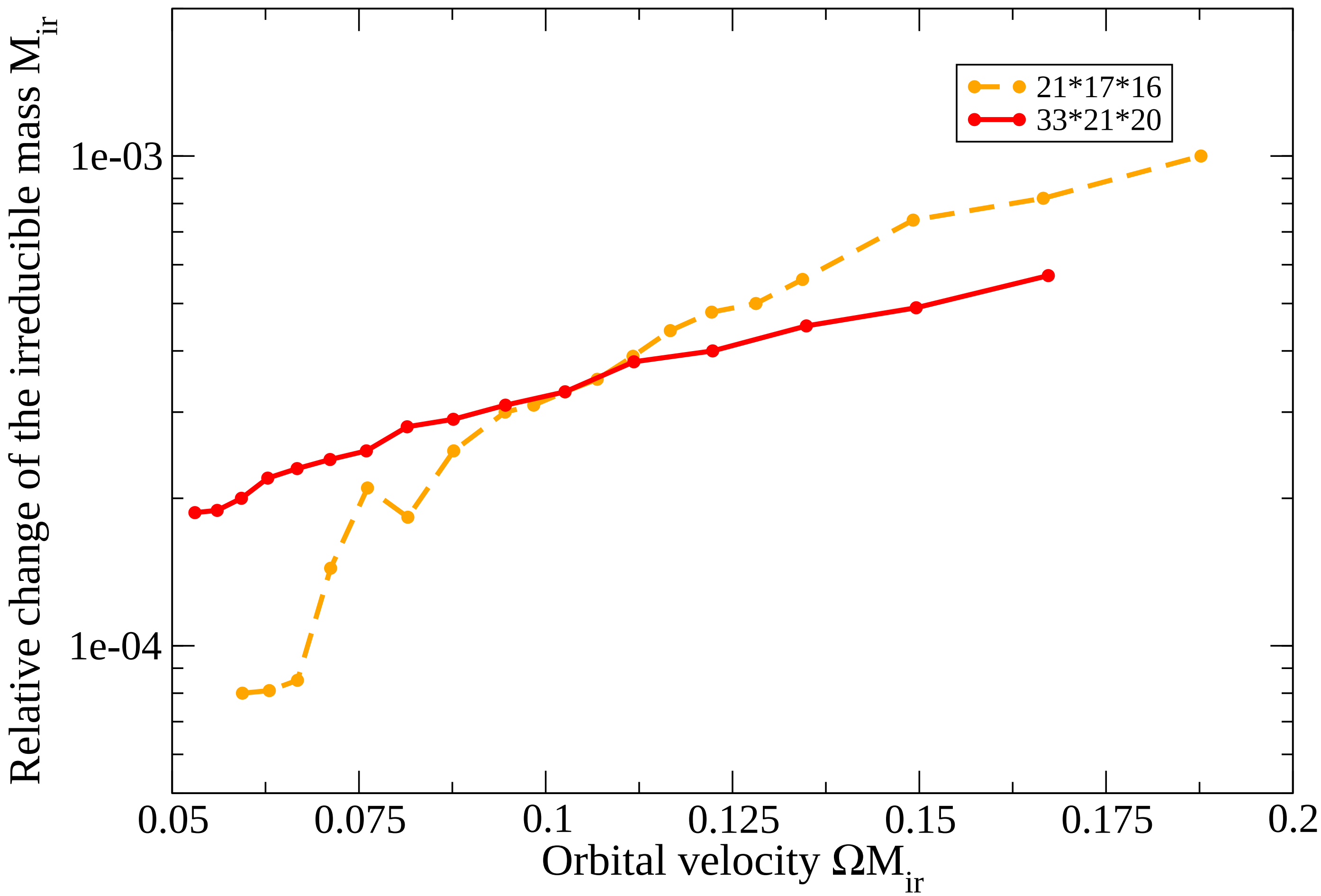

Relative change of the horizon area along an evolutionary sequence

Lapse in the orbital plane

ISCO configuration

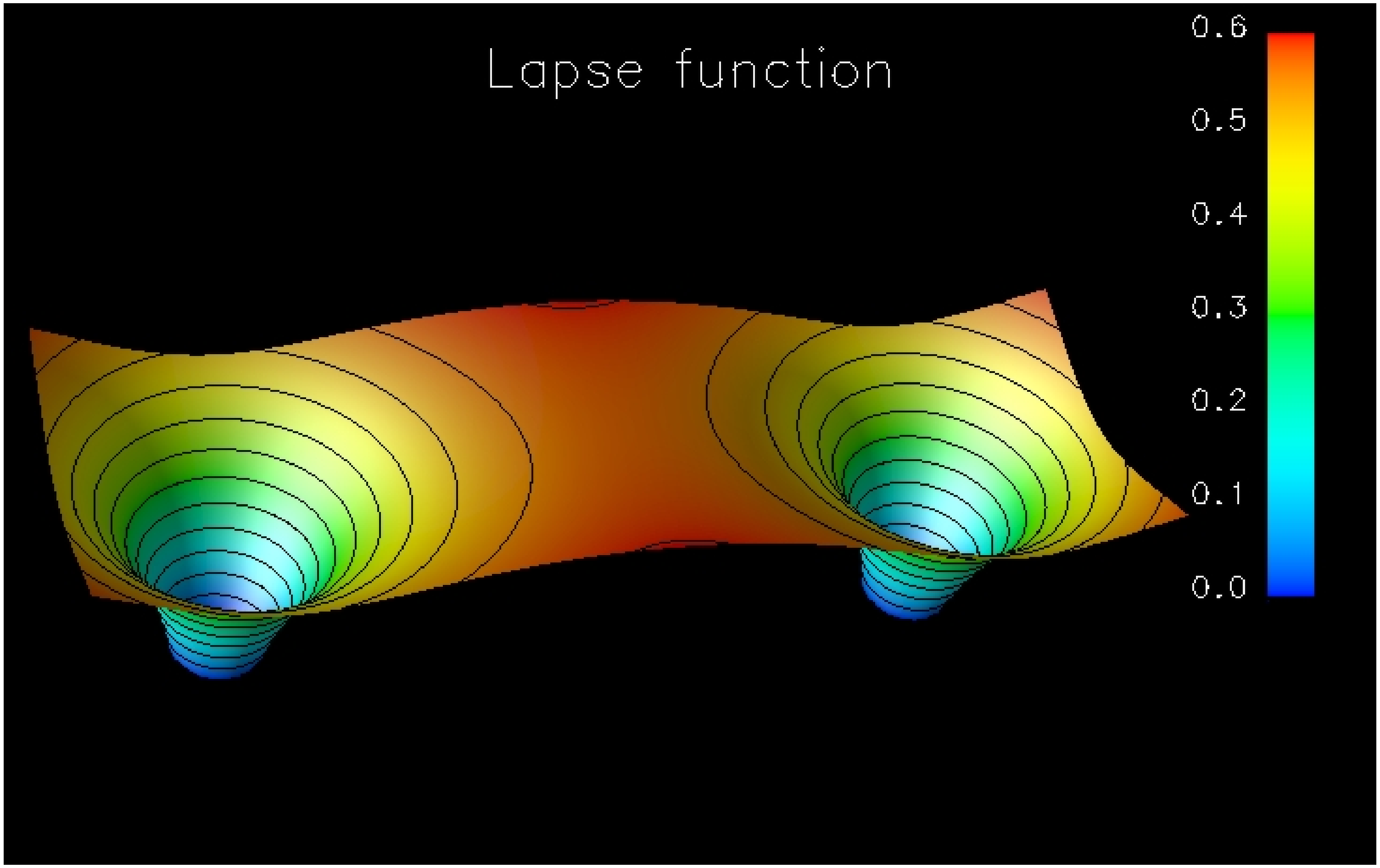

Lapse in the orbital plane

ISCO configuration

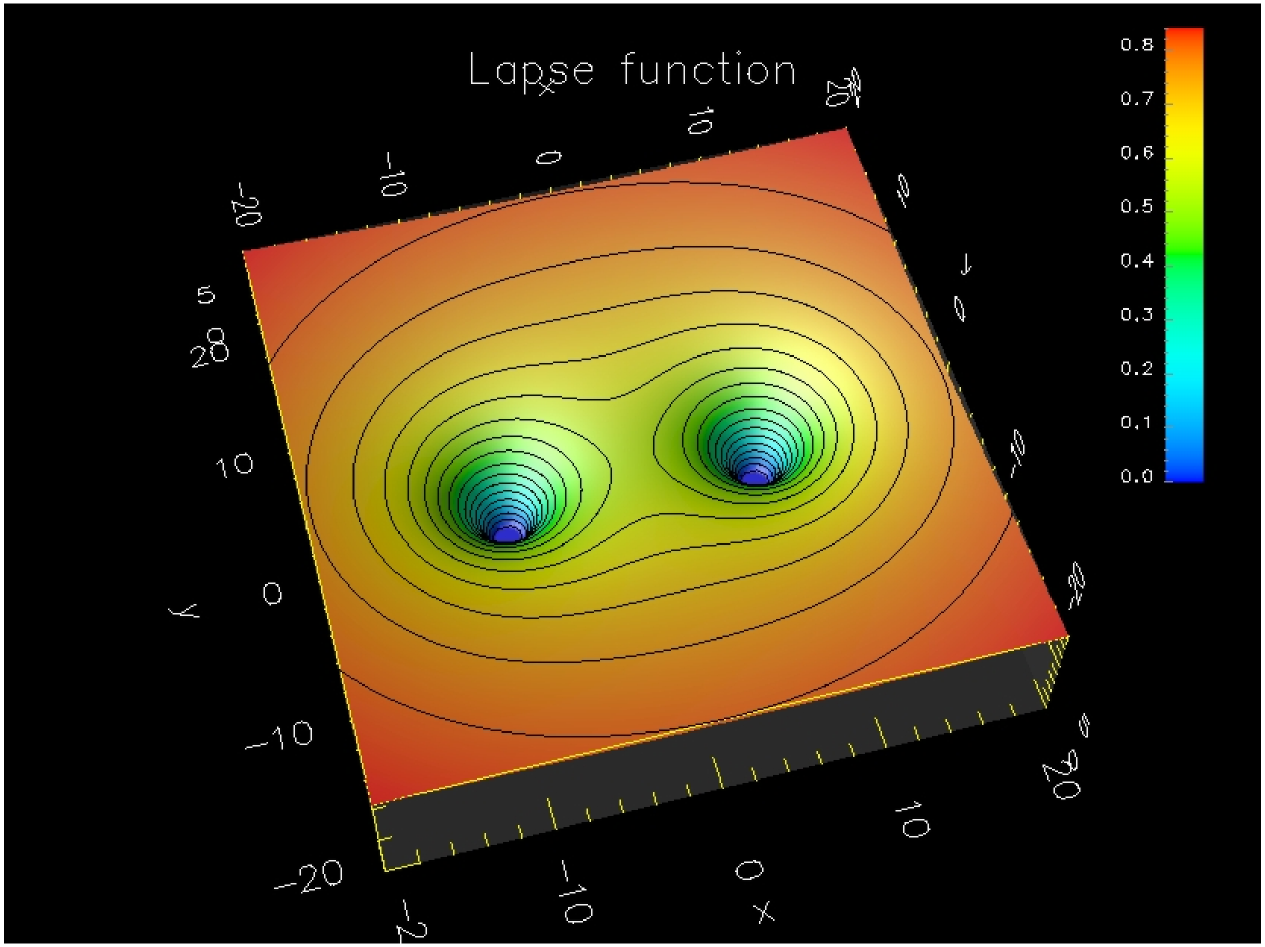

Shift vector in the orbital plane

ISCO configuration

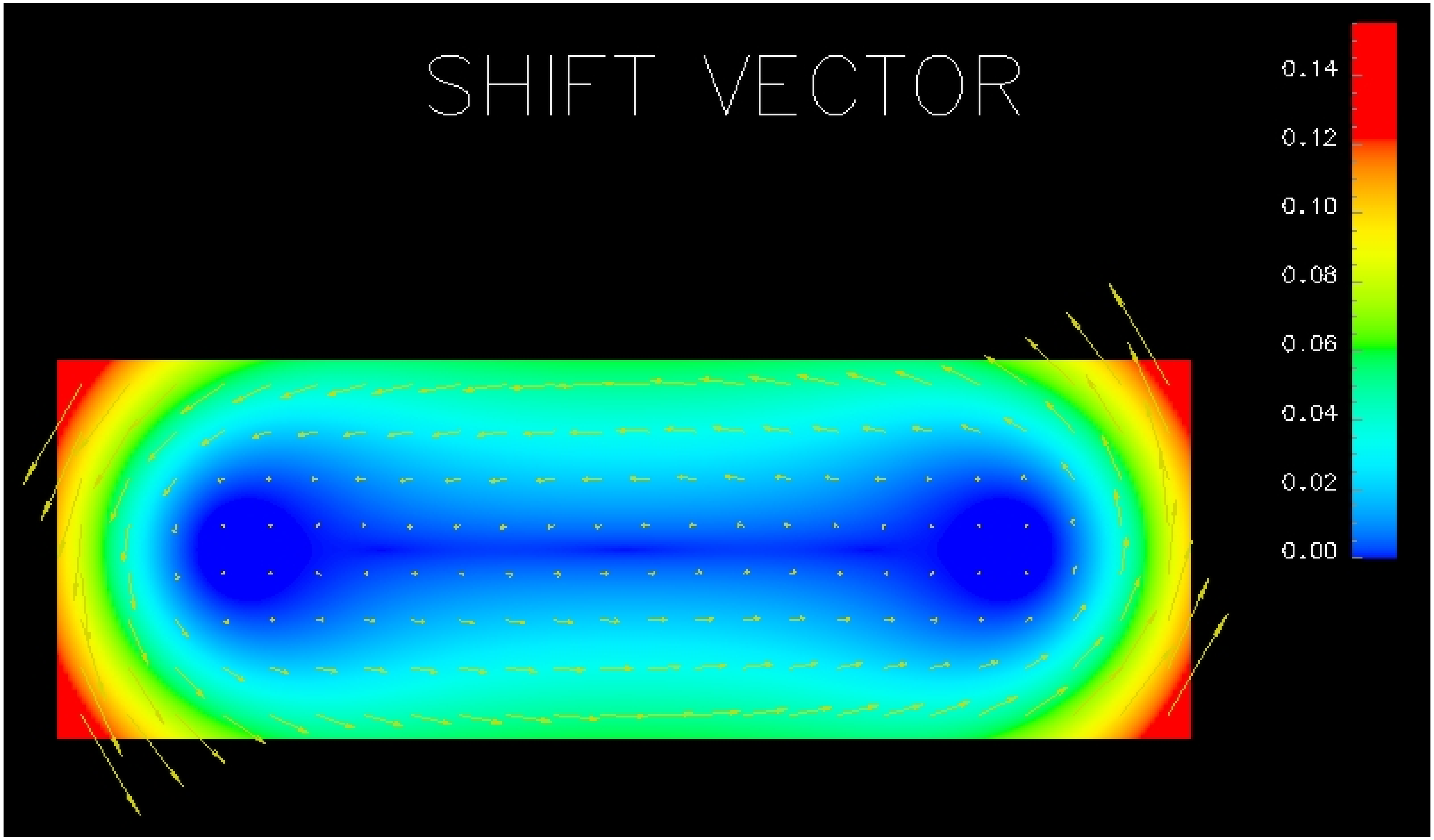

Conformal factor in the orbital plane

ISCO configuration

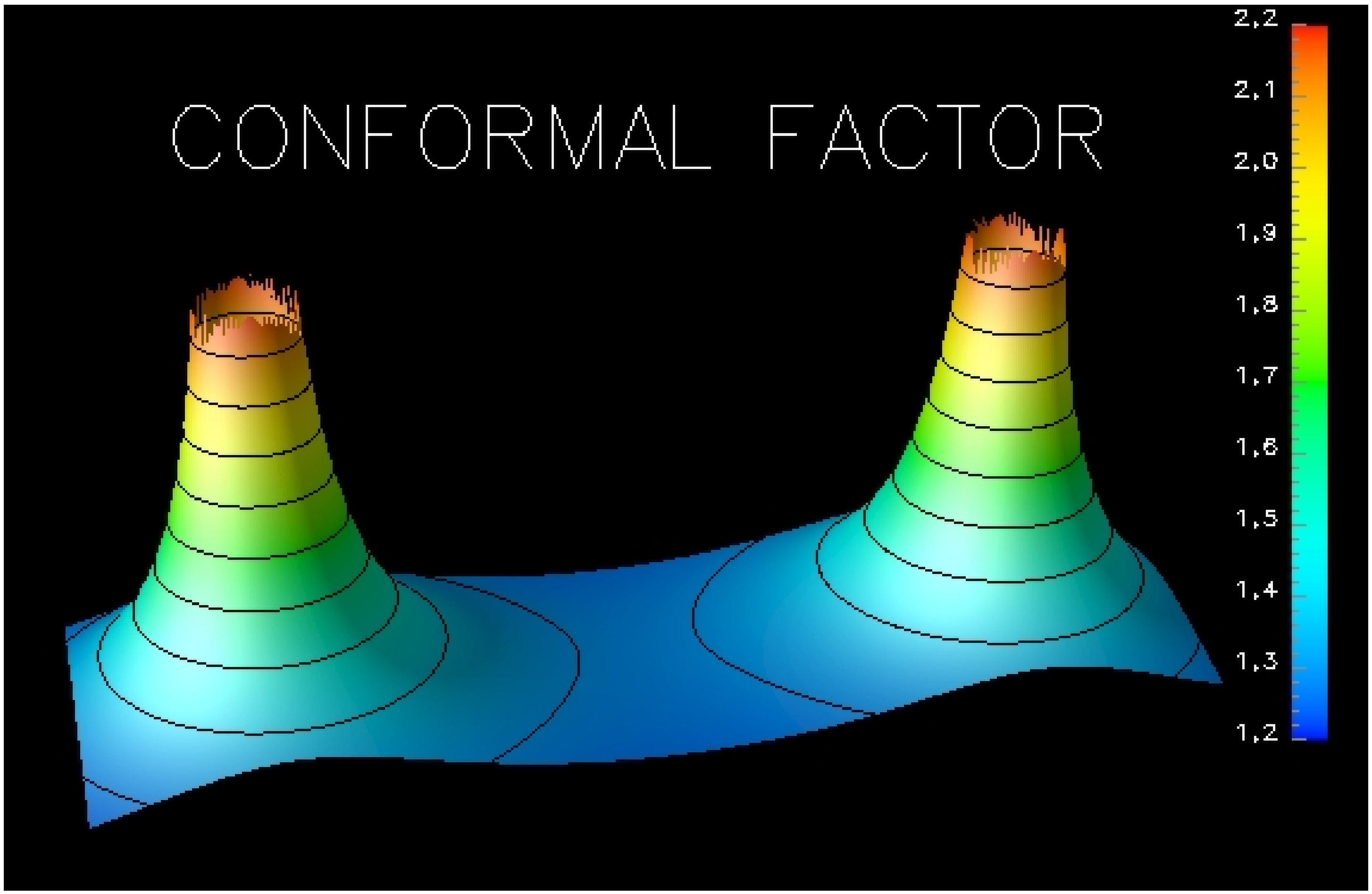

Extrinsic curvature in the orbital plane

ISCO configuration

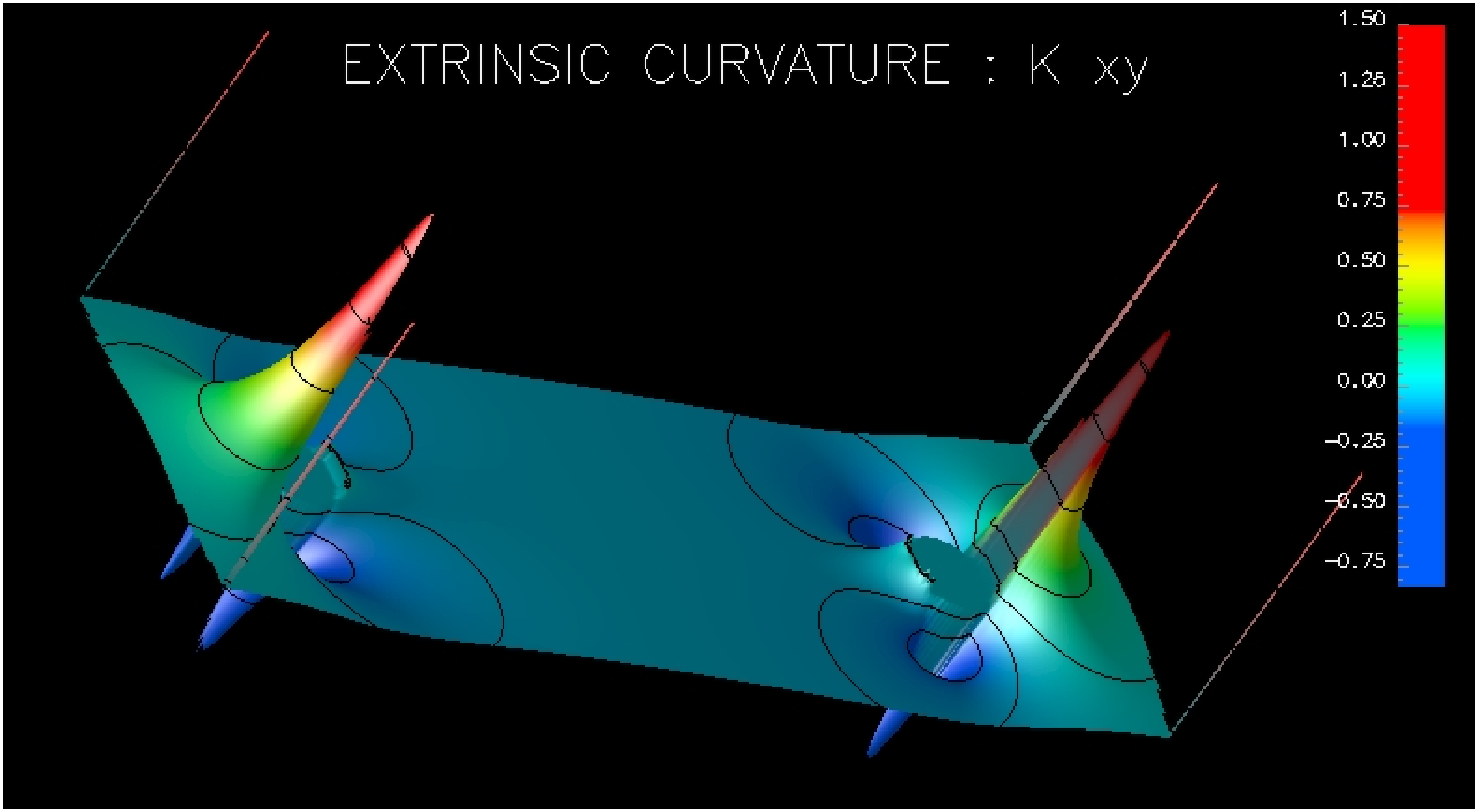

Evolutionary sequence

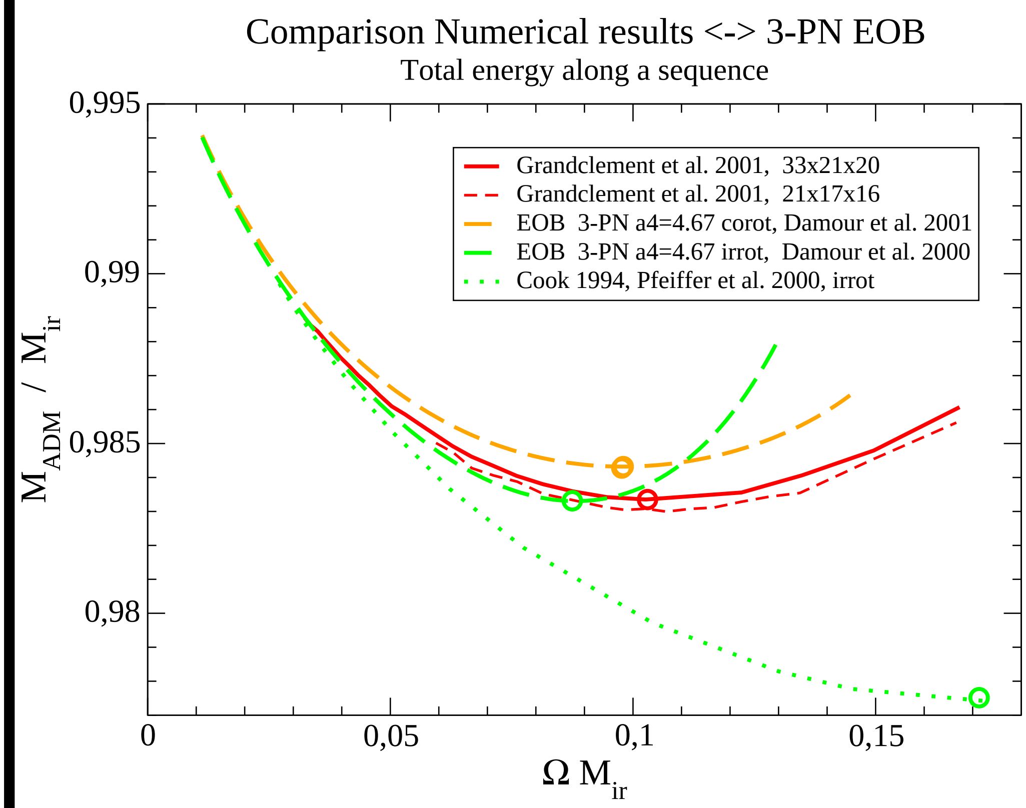

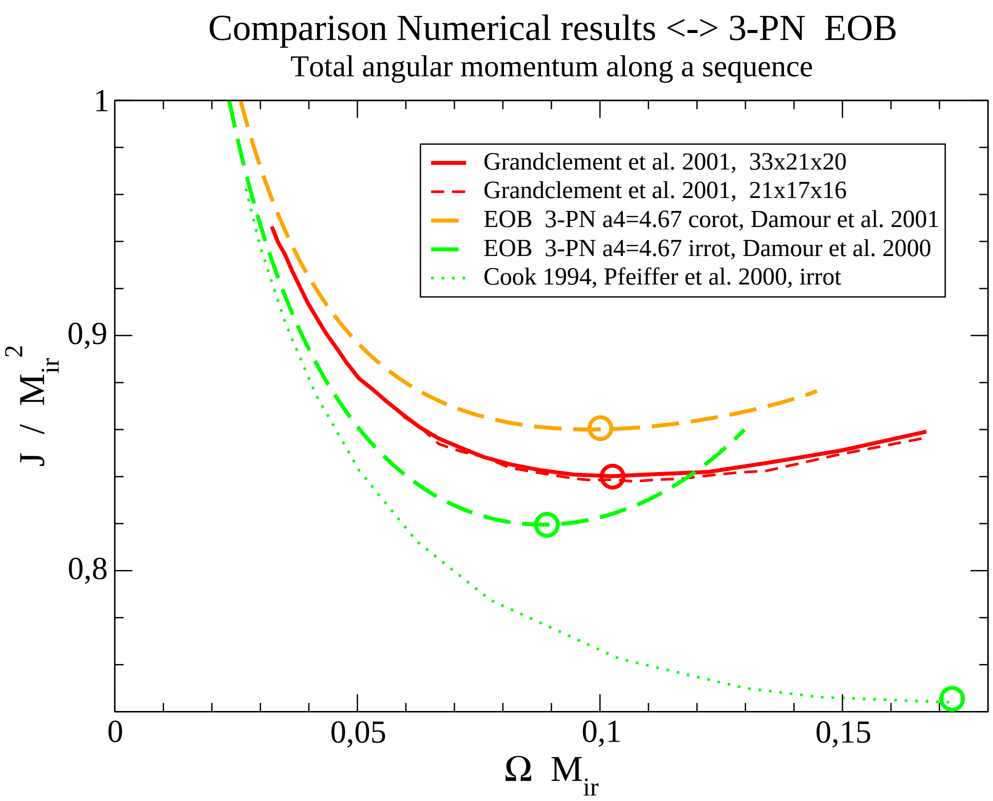

Location of the ISCO

Comparison with other methods